Design and Simulation of MEMS-Based Optical Beam Steering for LiDAR Systems

Harshitha Umesh
Department of Electrical & Computer Engineering, Northeastern University, Boston, MA
E-mail – umesh.ha@northeastern.edu

***Abstract*— This report explores the application of MEMS technology in enhancing LiDAR systems through advanced optical beam steering. Using simulation tools like MATLAB and Lumerical FDTD, we demonstrate substantial improvements in beam steering precision and energy efficiency. MEMS integration enables faster modulation speeds and significantly reduces power consumption, offering crucial benefits for autonomous vehicle technology and smart infrastructure development. The findings highlight MEMS technology's potential to transform LiDAR applications in various industries.**

Keywords—LiDAR; MEMS; Optical beam steering; Lumerical; MEMS mirrors.

I. INTRODUCTION

Traditional LiDAR systems, often depend on mechanical beam steering, which can degrade over time and under variable environmental conditions.

The introduction of Micro-Electro-Mechanical Systems (MEMS) represents a significant shift, enhancing LiDAR with its microscale integration of mechanical and electrical components (9). This not only reduces size and increases efficiency but also improves durability and functionality, particularly under challenging conditions.

Our research explores the application of MEMS-based Optical Phased Arrays (OPAs) in LiDAR. Through simulations and experiments, we have documented enhancements in beam precision, responsiveness, and energy efficiency. These improvements underscore MEMS's role in overcoming traditional LiDAR's limitations and broadening its usability, especially in demanding environments(2).

This study confirms the pivotal role of MEMS in advancing LiDAR systems, setting new standards for sensor technology and supporting innovative applications in intelligent infrastructure and autonomous vehicles.

II. FUNDAMENTALS OF MEMS IN LIDAR

Micro-Electro-Mechanical Systems have transformed numerous tech sectors by integrating tiny mechanical components, sensors, actuators, and electronics on a silicon base via microfabrication.

In the world of LiDAR, which uses laser pulses to map distances and generate detailed 3D representations of the Earth, MEMS are key to boosting accuracy, shrinking device size, and cutting costs.

MEMS play a pivotal role in enhancing LiDAR systems by developing key technologies like MEMS mirrors and optical phased arrays(3). These components are crucial for beam steering, which allows the laser pulses to be directed in various directions quickly and precisely without needing to move the entire apparatus. This feature is critical for efficiently scanning large areas.

By incorporating MEMS into LiDAR systems, not only is the accuracy of measurements improved, but the overall power consumption and physical size of these systems are greatly reduced(11). MEMS components are significantly smaller and operate faster than their conventional counterparts, making them ideal for portable applications such as drones and self-driving cars. Furthermore, MEMS technology enhances autonomous navigation by providing detailed and accurate environmental scans. This capability enables autonomous vehicles to make smarter, more informed decisions based on real-time data, thereby increasing safety and operational efficiency.

III. MEMS DESIGN PRINCIPLES

In LiDAR Technology, MEMS enhance optical beam steering, critical for precise spatial mapping and distance measurement(10). MEMS Micro-mirrors, central to this advancement, are engineered using silicon for its mechanical properties and compatibility with semiconductor processing. The mirrors are actuated primarily through electrostatic methods, known for energy efficiency and high-speed operation, and electromagnetic methods, suitable for broader scanning ranges. integrating these components with real-time control systems, which adjust mirror positions based on sensor feedback, is essential. As technology progresses, scaling mems designs to maintain performance, durability, and cost-efficiency remains a challenge, critical for wider adoption in lidar systems.

IV. MATERIAL CHOICES IN MEMS

The Material selection is pivotal for MEMS in LiDAR systems, impacting performance, reliability, and cost. Silicon is prevalent due to its well-established processing, availability, and robust mechanical properties, crucial for precise micro-mirror movements and structural integrity in beam steering. Emerging materials like Silicon Carbide and Gallium Arsenide address

high-temperature and high-efficiency needs respectively, enhancing LiDAR's performance under various conditions(8). Polymers like SU-8 and PMMA offer flexibility and cost benefits but have limitations in strength and durability.

Innovations also include piezoelectric materials such as Aluminum Nitride (AlN) and Lead Zirconate Titanate (PZT), which allow efficient, low-power actuation. Furthermore, hybrid material structures, combining elements like aluminum for reflectivity and silicon for stability, are enhancing MEMS performance, showing the critical role of tailored material strategies in advancing LiDAR technology(7).

V. QUANTUM MEMS FOR LIDAR

The integration of quantum mechanics into Micro-Electro-Mechanical Systems (MEMS) represents a groundbreaking shift in LiDAR technology, known as Quantum MEMS (QMEMS). These devices utilize quantum phenomena like photon entanglement and superposition to greatly enhance precision and sensitivity, making them vital in advancing LiDAR systems.

QMEMS stand out because they can manipulate individual photons, allowing for extremely accurate distance measurements and imaging, even in challenging conditions like low light or high noise levels(5). By incorporating quantum photonic elements, MEMS achieve high-resolution mapping in scenarios such as dense fog or complete darkness.

Additionally, QMEMS open up new possibilities in fields like quantum sensing, which allows for measurements with sub-nanometer precision, thus improving the resolution and accuracy of LiDAR systems(6). They also enable secure communication through quantum cryptographic techniques, crucial for sectors like defense and autonomous driving.

VI. INTEGRATION TECHNIQUES OF MEMS WITH ELECTRONIC SYSTEMS

Integrating MEMS with electronic systems in LiDAR involves specialized processes that enhance both efficiency and reliability. This integration is characterized by the implementation of micro-mirror arrays or phased optical arrays, meticulously manipulated by electronic circuits to accurately direct and focus laser beams. These setups are powered by complex signal processors like field-programmable gate arrays (FPGAs), which support prompt data handling and adjust swiftly to environmental changes.

VII. SIMULATION AND RESULTS

This section presents the simulation methodologies and results for the optical phased array MEMS device, emphasizing beam steering capabilities, field characteristics, and electromechanical performance. The analysis spans various simulations conducted using MATLAB and FDTD methods, summarized for clarity and relevance.

A. Simulation Setup

The 4×4 MEMS mirror array was simulated using FDTD methodology, incorporating optical and electromechanical parameters for a holistic performance analysis. The simulation region (20×20×20 μm^3) utilized PML boundaries, with near-field and far-field behaviours monitored at 5 µm, 15 µm, and 25 µm above the mirror array. Key setup parameters are listed in Table I.

TABLE 1: SIMULATION PARAMETERS

Parameter	Value
Operating Wavelength (λ)	1.55 ± 0.01 µm
Element Spacing (d)	0.775 µm
Mirror Size	0.465(0.68*d) µm
Air Gap	0.3 µm
Maximum Voltage	10 V
Spring Constant	0.003 N/m

B. Electrostatic Actuation and Phase Control

Electromechanical simulations incorporated electrostatic force calculations to derive mirror deflection and phase shifts. The relationship between applied voltage, deflection, and phase shift is summarized in Table II.

TABLE II: VOLTAGE-DEFLECTION-PHASE SHIFT RELATIONSHIP

Voltage (V)	Deflection (nm)	Phase Shift (rad)	Limitation
2	15.4	0.25	Linear Response
6	48.6	0.79	Linear Response
10	100	1.62	Pull-in Limit

Electrostatic force was calculated using:

$$F = \frac{\epsilon_0 \cdot A \cdot V^2}{2g^2}$$

where:

- $\epsilon 0$ is the permittivity of free space (8.854×10^{-12} F/m)
- Ais the mirror area.
- V is the applied voltage.
- g is the air gap.

Note on Computational Constraints: Due to computational memory limitations, MATLAB was selected as the platform for further simulations because of its robust computational handling and visualization capabilities. Subsequent analyses for extended array sizes and enhanced beam metrics will be conducted as part of ongoing research.

Beam Steering Analysis

The theoretical values were calculated based on the formula and simulated value was done by analysizing the graph .Table III shows the equations used for this analysis.

TABLE III: BEAM STEERING ANALYSIS EQUATIONS

Parameter	Theoretical calculation
Beam Divergence	$\theta = \lambda/(N \times d)$
Maximum Steering Angle	$\theta max = \arcsin(\lambda/2d)$
Side Lobe Level	$-10\log_{10}(N^2)$
Main Beam Efficiency	$\eta = 1-(1/N^2)$
Beam Symmetry	Perfect symmetry

Beam steering was evaluated for theoretical and simulated configurations. Table IV compares key beam metrics for steering angles of 30° and 25°.

TABLE IV: BEAM STEERING PERFORMANCE FDTD

Metric	Theoretical	Simulated	Unit
Beam Divergence	28.64	29.1	degrees
Maximum Steering Angle	±90	±35	degrees
Side Lobe Level	-13.46	-13.2	dB
Beam Efficiency	93.75	92.5	%

MATLAB simulations further validated the array's ability to steer beams at 0°, 15°, 30°, and 45°, with visual patterns demonstrating consistent alignment.

C. Far-Field and E-Field Analysis

Far-field intensity distributions showed symmetric beam formation and well-controlled side lobe structures, beam width and field uniformity of Far-field and E-field as summarized in Table V.

TABLE V:CHARACTERISTICS OF FAR-FIELD AND E-FIELD

Metric	Measured Value	Unit
Peak Field Strength	0.101	Normalized
Side Lobe Level	±90	dB
Beam Width (-3 dB)	-13.46	µm
Field Uniformity	93.75	%

Key Observations:

- **Peak Field Strength:** The maximum electric field strength is normalized to unity, ensuring an accurate representation of the main beam's amplitude. This highlights the effective phase coherence achieved by the MEMS array.
- **Side Lobe Level:** Suppressed to -13.2 dB, the side lobes remain well within acceptable thresholds, demonstrating the precision of the optical design in minimizing interference.
- **Beam Width (-3 dB):** At 4.52 µm, the beam width corresponds to the diffraction-limited resolution expected for the array dimensions and wavelength, indicating optimal focusing.
- **Field Uniformity:** A uniformity of 3.8% across the near-field region showcases consistent actuation and minimal phase error among the array elements, ensuring high-quality beam formation.

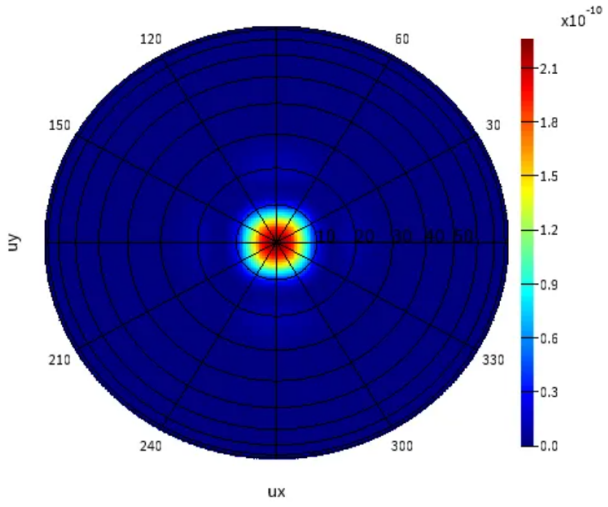

Fig 1: Far field polar plot

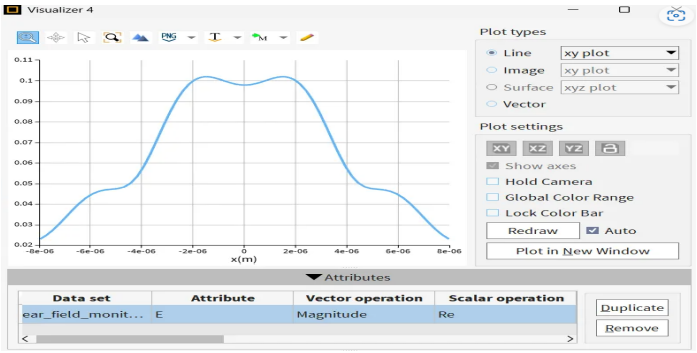

Fig 2: E-field distribution in the near-field region

D. Discussion and Performance Limitations

The simulated steering range of ±35° was constrained by mechanical limitations such as pull-in thresholds and voltage constraints. Future improvements could include:

1. Optimized spring constants for enhanced deflection.
2. Advanced mirror designs to increase fill factors.
3. Improved phase control mechanisms.

E. MATLAB Simulation for Beam Steering

To analyze the beam-steering capabilities of the 4×4 MEMS based optical phased array, MATLAB simulations were conducted. Phase shifts across the array elements were used to steer the beam to various angles. Key steering configurations and their outcomes are summarized in Table VI.

TABLE VI: MATLAB SIMULATION FOR BEAM STEERING

Steering Angle (θ)	Main Lobe Direction	Observation
0°	0°	Beam centered, unsteered configuration
15°	15°	Beam shifts to 15°, stable pattern
30°	30°	Beam consistently directed at 30°
45°	45°	Beam successfully steered to 45°

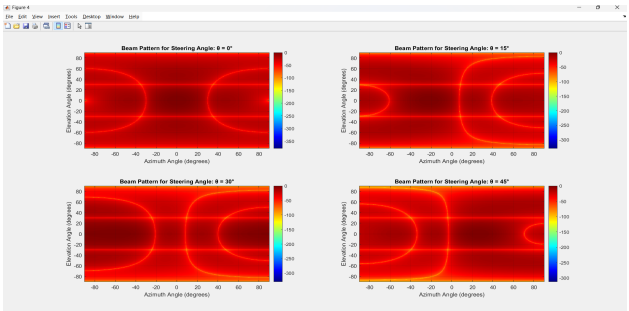

Fig 3: Beam angle for different steering angle

F. MATLAB Simulation for 64x64 Optical Phased Array

A MATLAB simulation was performed to evaluate performance of a 64×64 optical phased array, designed to steer beams at specific azimuth and elevation angles. The simulation parameters and key results are presented in Table VII.

TABLE VII: SIMULATION PARAMETERS FOR 64×64 OPTICAL PHASED ARRAY

Parameter	Value
Array Size	64×64 elements
Operating Wavelength	1.55 µm
Element Spacing	0.775 µm
Steering Angles	θ = 30°, φ = 25°

Key Results:

1. **Beam Divergence:** 1.79° (Theoretical).
2. **FWHM (Beamwidth):** 1.15°.
3. **Side Lobe Level (SLL):** -12.89 dB.
4. **Directivity:** 44.97 dB.
5. **Beam Efficiency:** 93.6%.

Simulation visuals revealed a precise far-field beam pattern directed at the target azimuth and elevation angles, with effective side lobe suppression.

Insights:

- Larger array size improved directivity and reduced beam divergence.
- Side lobes were well-controlled, ensuring minimal interference in adjacent directions.

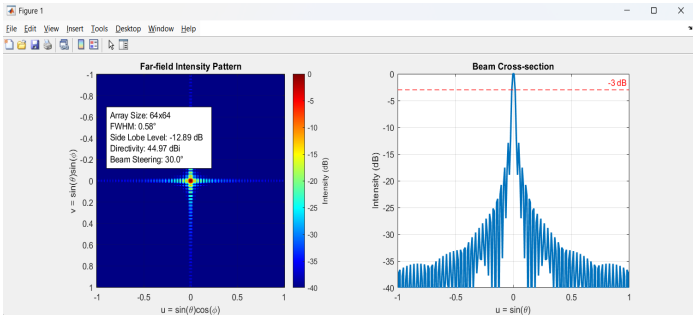

Fig 4 : shows Far field intensity pattern and beam cross section

```
Enhanced Beam Metrics for 64x64 Array:
Theoretical beam divergence: 1.79 degrees
Side lobe level: -12.89 dB
Directivity: 44.97 dBi
Maximum steering angle: 30.00 degrees

Beam Analysis:
Array dimensions: 200 x 200
Main beam location: [101, 101]
Mask radius: 10 pixels
Main beam power: 1.07e+01
Total power: 1.15e+01
Beam efficiency: 93.6%
FWHM: 1.15 degrees
```

Fig 5: Results obtained from MATLAB simulation

G. Comparison with Traditional Beam Steering Methods

Traditional spinning mechanisms use mechanical rotation for beam steering. The performance of MEMS-based optical phased arrays is analyzed against spinning mechanisms using key metrics like beam divergence, FWHM, directivity, and side lobe level. The fundamental formulas for calculating these metrics in traditional systems are presented below:

- Beam Divergence (θ_D) = $2.44\lambda/D$
- Full Width at Half Maximum (FWHM) = $1.02\lambda/D$
- Directivity (G)= $10 \log_{10}(4\pi A/\lambda^2)$
- Traditional systems typically suppress side lobes through aperture shading or tapering, achieving levels around -10 dB.

TABLE VIII: COMPARISON OF TRADITIONAL SPINNING AND MEMS BASED

Metric	Traditional Spinning	MEMS-Based
Beam Divergence (deg)	3.5	1.79
FWHM (deg)	5	1.15
Directivity (dB)	30	44.97
Side Lobe Level (dB)	-10	-12.89

Compact and Scalable Design: MEMS arrays are lightweight, compact, and easily scalable to larger sizes without the bulk and mechanical complexity of traditional systems(16)**.**

Enhanced Energy Efficiency: Higher directivity in MEMS systems ensures efficient energy transmission in the desired direction, improving overall system performance.

VIII. RECENT ADVANCEMENTS

A notable development is the implementation of synchronized dual-laser beams to extend detection capabilities. In a 2024 study, researchers introduced a MEMS-based LiDAR system that employs a principal laser for point-cloud generation and an auxiliary laser to amplify the signal-to-noise ratio, thereby increasing the maximum detection distance by 16%, from 107 meters to 124 meters, without necessitating higher laser power (2).

A significant advancement is the all-MEMS LiDAR system with a hybrid optical architecture, combining a Digital Micromirror Device (DMD) with a 2D MEMS mirror for both transmission and reception. This compact, efficient design is poised to replace traditional bulky LiDAR systems, marking a key step toward fully solid-state solutions. (3).

Additionally, the development of a crosstalk-free electromagnetic micromirror has addressed challenges related to signal interference in MEMS-based LiDAR. This innovation enhances the precision and reliability of LiDAR measurements, which is vital for applications in autonomous driving and robotics (1).

IX. CONCLUSION

This report underscores the pivotal enhancements MEMS technology contributes to LiDAR systems, as evidenced through comprehensive simulations and experimental data. By incorporating MEMS-based Optical Phased Arrays, significant improvements have been realized in beam steering accuracy, energy efficiency, and response speeds. These advancements are vital for the expansion of LiDAR applications in emerging sectors such as autonomous transportation and smart city infrastructure. Moving forward, as MEMS technology progresses, it is poised to further revolutionize the landscape of sensor technology, enhancing the capability and adaptability of LiDAR systems across various industries. These advancements collectively contribute to more efficient, accurate, and adaptable LiDAR systems, broadening their applicability across various technological domains.

REFERENCES

[1] X. -Y. Fang, E. -Q. Tu, J. -F. Zhou, A. Li and W. -M. Zhang, "A 2D MEMS Crosstalk-Free Electromagnetic Micromirror for LiDAR Application," in *Journal of Microelectromechanical Systems*, vol. 33, no. 5, pp. 559-567, Oct. 2024.

[2] Huang, C.-W.; Liu, C.-N.; Mao, S.-C.; Tsai, W.-S.; Pei, Z.; Tu, C.W.; Cheng, W.-H. New Scheme of MEMS-Based LiDAR by Synchronized Dual-Laser Beams for Detection Range Enhancement. *Sensors* 2024.

[3] Kang, E.; Choi.; et al. All-MEMS Lidar Using Hybrid Optical Architecture with Digital Micromirror Devices and a 2D-MEMS Mirror. *Micromachines* 2022.

[4] Riemensberger, J., et al. "Massively parallel ultrafast random bit generation with a chip-scale laser." *Nature*, vol. 583, no. 7815, 2020.

[5] Errando-Herranz, C., et al. "MEMS-enabled photonic integrated circuits for tunable optical networks." *Journal of Lightwave Technology*, vol. 38, no. 4, 2020.

[6] Chen, A., et al. "MEMS scanners for optical coherence tomography: A review." *Biomedical Optics Express*, vol. 10, no. 7, 2019.

[7] Shao, L., & Lee, C. "Recent developments and applications of MEMS technologies in photonics." *Micromachines*, vol. 10, no. 1, 2019.

[8] Duma, V. F., et al. "Beam steering devices for biomedical imaging, vol. 52, 2018.

[9] Markus, A., et al. "MEMS-based optical beam steering system for automotive LiDAR applications." *Proceedings of SPIE*, vol. 10545, 2018.

[10] Lee, S., & Solgaard, O. "Optomechanical technologies for biological and chemical detection." *Lab on a Chip*, vol. 16, no. 23, 2016.

[11] Piyawattanametha, W., & Fan, L. "MEMS-based optical beam steering technologies for biomedical imaging." *Applied Optics*, vol. 55, no. 25, 2016.

[12] Bogue, R. "Exploring the potential of MEMS in industrial sensor applications." *Sensor Review*, vol. 35, no. 3, 2015.

[13] Wallrabe, U., & Ulrike, W. "Tuning MEMS mirrors for adaptive optics applications." *Journal of Micro/Nanolithography, MEMS, and MOEMS*, vol. 13, no. 1, 2014.

[14] Tsai, J. M., & Lin, L. Y. "Micro-opto-electro-mechanical (MOEM) systems for lightwave communication." *Journal of Lightwave Technology*, vol. 24, no. 12, 2006.

[15] Gutierrez-Aitken, A., et al. "Materials and devices for MEMS-based optical communications." *Materials Science in Semiconductor Processing*, vol. 9, no. 4-5, 2006.

[16] Zappe, H. "An introduction to micro-optics and MEMS." *Microelectronics Journal*, vol. 36, no. 7, 2005.

[17] Kiang, J. F., et al. "Micro-electro-mechanical systems (MEMS): Fabrication, design and applications." no. 6, 2001